ELSEVIER

Contents lists available at ScienceDirect

Journal of Chromatography A

journal homepage: www.elsevier.com/locate/chroma



Development of peptide ligands for the purification of α -1 antitrypsin from cell culture fluids



Wenning Chu^{a,*}, Raphael Prodromou^a, Brandyn Moore^a, Driss Elhanafi^b, Ryan Kilgore^a, Shriarjun Shastry^{a,b}, Stefano Menegatti^{a,b,c,*}

- ^a Department of Chemical and Biomolecular Engineering, North Carolina State University, 911 Partners Way, Raleigh, NC 27606
- ^b Biomanufacturing Training and Education Center (BTEC), North Carolina State University, 850 Oval Dr. Raleigh, NC 27606
- ^c LigaTrap Technologies LLC, Durham, NC 27701

ARTICLE INFO

Article history: Received 2 June 2022 Revised 19 July 2022 Accepted 20 July 2022 Available online 22 July 2022

Keywords: α -1 antitrypsin Peptide ligands Affinity chromatography Protein purification CHO cell culture harvest

ABSTRACT

 α -1 antitrypsin (AAT) deficiency, a major risk factor for chronic obstructive pulmonary disease, is one of the most prevalent and fatal hereditary diseases. The rising demand of AAT poses a defined need for new processes of AAT manufacturing from recombinant sources. Commercial affinity adsorbents for AAT purification present the intrinsic limitations of protein ligands - chiefly, the high cost and the lability towards the proteases in the feedstocks and the cleaning-in-place utilized in biomanufacturing - which limit their application despite their high capacity and selectivity. This work presents the development of small peptide affinity ligands for the purification of AAT from Chinese hamster ovary (CHO) cell culture harvests. An ensemble of ligand candidates identified via library screening were conjugated on Toyopearl resin and evaluated via experimental and in silico AAT-binding studies. Initial ranking based on equilibrium binding capacity indicated WHAKKSKFG- (12.9 mg of AAT per mL of resin), WHAKKSHFG- (16.3 mg/mL), and KWKHSHKWG- (15.8 mg/mL) Toyopearl resins as top performing adsorbents. Notably, the fitting of adsorption data to Langmuir isotherms concurred with molecular docking and dynamics in returning values of dissociation constant (K_D) between 1 – 10 μ M. These peptide-based adsorbents were thus selected for AAT purification from CHO fluids, affording values of AAT binding capacity up to 13 gram per liter of resin, and product yield and purity up to 77% and 97%. WHAKKSHFG-Toyopearl resin maintained its purification activity upon 20 consecutive uses, demonstrating its potential for AAT manufacturing from recombinant sources.

© 2022 Elsevier B.V. All rights reserved.

1. Introduction

 α -1 antitrypsin (AAT) deficiency is an inherited disorder that frequently causes chronic obstructive pulmonary (COPD) and liver diseases, and - more rarely - inflammation of the skin (panniculitis) or blood vessels (vasculitis) [1,2]. AAT deficiency occurs worldwide, although its prevalence varies by population, and affects about 1 in 1500 to 3500 individuals with European ancestry [3]. Augmentation therapy, otherwise called replacement therapy, is a treatment available to patients with AAT deficiency and aims to increase the blood level of AAT by supplementing the purified human protein by intravenous infusion [4].

Current AAT manufacturing processes utilize human plasma as a source, owing to its wide availability, in particular its Cohn Fraction IV precipitate: the cleavage of disulfide bonds of all proteins

E-mail addresses: wchu3@ncsu.edu (W. Chu), smenega@ncsu.edu (S. Menegatti).

in Fraction IV using a reducing reagent, typically dithiothreitol, followed the centrifugation of the resulting precipitate affords an AAT-enriched solution that is suitable for chromatographic purification [5]. However, the complexity of plasma fractionation, the loss of proteins during AAT enrichment from Cohn fraction IV, the need of subsequent chromatographic processing, and the risk of transmitting infectious agents from pooled plasma to the AATD patients limit the attractiveness of this process [6].

The recent advancements in engineering cell lines capable of protein expression and secretion at high titer point towards recombinant production as a viable alternative to meet the clinical demand of human AAT [7]. This places the focus on the downstream pipeline and the availability of robust chromatographic adsorbents enabling affordable purification at scale.

Currently, Alpha-1 Antitrypsin Select – henceforth, AAT Select – is the only affinity resin commercially available for AAT purification [8]. By relying on a camelid antibody fragment for AAT capture, this resin features high binding capacity (\sim 10 mg of AAT per mL

^{*} Corresponding authors.

of resin, [9,10]) and selectivity; however, it also presents the characteristic limitations of affinity absorbents functionalized with protein ligands, namely high cost and lability towards the proteases in the feedstocks and caustic cleaning-in-place, which can cause the release of immunogenic fragments in the product stream and shorten the resin's lifetime [11].

Responding to these challenges, in this study we present the discovery and development of AAT-binding peptides for use as affinity ligands in AAT purification. To this end, we initially designed a focused library of peptides, whose amino acid composition and sequence length was informed by the in silico analysis of α -helices A – E of AAT. These form the core structure of AAT and, being removed from the reactive center loop (RCL) [12], represents an ideal binding site for AAT capture. The peptide library was screened by implementing a dual-fluorescent selection method developed in prior work [13-17], which combines microfluidic technology and real time image analysis to accelerate the identification of candidate sequences and minimize the risk of false positives. A set of 15 candidate peptide ligands was conjugated onto polymethacrylate-based Toyopearl resins, and evaluated in terms of AAT dynamic binding capacity and purification from a Chinese hamster ovary (CHO) cell culture supernatant. Ligands WHAKKSKFG, WHAKKSHFG, and KAWFKHWNG featured remarkable values of binding capacity, rivaling the control AAT Select resin. Adsorbent WHAKKSHFG-Toyopearl resin afforded high values of AAT yield and purity, and maintained an excellent purification performance upon repeated usage, demonstrating its potential for AAT manufacturing from recombinant sources.

2. Experimental

2.1. Materials

Aminomethyl ChemMatrix and HMBA-ChemMatrix (particle diameter: 75-150 µm, loading: 0.6 mmol per g resin) resins were sourced from PCAS Biomatrix, Inc. (Saint-Jean-sur-Richelieu, Quebec, Canada). The Toyopearl AF-Amino-650 M resin was obtained from Tosoh Corporation (Tokyo, Japan). NHS-AlexaFluor 488 (AF488) and NHS-AlexaFluor 594 (NHS-AF594), N,N'-dimethylformamide (DMF), dichloromethane (DCM), methanol, and N-methyl-2-pyrrolidone (NMP) were obtained from Fisher Chemical (Hampton, NH, USA). Fluorenylmethoxycarbonyl-(Fmoc-) protected amino acids Fmoc-Gly-OH, Fmoc-Ser(tBu)-OH, Fmoc-Ile-OH, Fmoc-Ala-OH, Fmoc-Phe-OH, Fmoc-Tyr(tBu)-OH, Fmoc-Asp(OtBu)-OH, Fmoc-His(Trt)-OH, Fmoc-Arg(Pbf)-OH, Fmoc-Lvs(Boc)-OH, Fmoc-Asn(Trt)-OH, and Fmoc-Glu(OtBu)-OH, Hexafluorophosphate Azabenzotriazole Tetramethyl Uronium (HATU), diisopropylethylamine (DIPEA), piperidine, and trifluoroacetic acid (TFA) were obtained from ChemImpex International (Wood Dale, IL, USA). Kaiser test kits, triisopropylsilane (TIPS), and 1,2ethanedithiol (EDT) were obtained from Millipore Sigma (St. Louis, MO, USA).

Null CHO-S clarified cell culture harvest was provided by BTEC (Raleigh, NC, USA). Human Alpha-1 antitrypsin (AAT) in lyophilized form was a gift of CSL Behring (King of Prussia, PA, USA). Glacial acetic acid, hydrochloric acid, sodium acetate, glycine, sodium hydroxide, potassium chloride, sodium chloride (NaCl), magnesium chloride (MgCl₂), Tris-HCl, Bis-Tris-HCl, ethanol, and dithiothreitol (DTT) were purchased from Fisher Scientific (Hampton, NH, USA). Phosphate buffered saline (PBS) at pH 7.4 was purchased from MilliporeSigma (St. Louis, MO, USA). Vici Jour PEEK chromatography columns (2.1 mm ID, 30 mm length, 0.1 mL volume), Alltech chromatography columns (3.6 mm ID, 50 mm length, 0.5 mL volume), and 10 µm polyethylene frits were obtained from VWR International (Radnor, PA, USA). All chromatographic experiments were performed using a ÄKTA Pure system from Cytiva (Marlbor-

ough, MA, USA). The BioResolve SEC mAb Column, 200 Å, 2.5 μ m, 7.8 \times 300 mm, size exclusion chromatography column was obtained from Waters Inc. (Milford, MA, USA). The AAT Select column was from Cytiva (Marlborough, MA). The 10–20% Tris-Glycine HCl SDS-PAGE gels and Coomassie blue stain were purchased from Bio-Rad Life Sciences (Carlsbad, CA, USA). A PierceTM BCA Protein Assay Kit and SilverQuestTM Silver Staining Kit were purchased from Fisher ScientificTM (Pittsburgh, PA, USA).

2.2. Synthesis of peptide libraries on aminomethyl Chemmatrix resin and selected peptides on Toyopearl resin

Peptide synthesis was performed on a Syro I automated peptide synthesizer (Biotage, Uppsala, Sweden) using nine protected amino acids, namely Fmoc-Ala-OH, Fmoc-Asn(Trt)-OH, Fmoc-Glu-(OtBu)-OH, Fmoc-Phe-OH, Fmoc-His(Trt)-OH, Fmoc-Lys(Boc)-OH, Fmoc-Ile-OH, Fmoc-Trp(Boc)-OH, and Fmoc-Ser(tBu)-OH: each amino acid coupling step was performed at 45 °C for 20 min, using 3 equivalents (eq.) of protected amino acid at the concentration of 0.5 M, 3 eq. of HATU (0.5 M), and 6 eq. of DIPEA (0.5 M) in 5 mL of dry DMF. The yield of peptide conjugation was monitored after each amino acid via the Kaiser test. The removal of Fmoc protecting groups was performed at room temperature using 20% v/v piperidine in DMF. The 6-mer peptide library X1-X2-X3-X4-X5-X6 and 8-mer peptide library X1-X2-X3-X4-X5-X6-X7-X8 were synthesized on 2 g of HMBA-ChemMatrix resin preloaded with the tripeptide spacer GSG (G: glycine; S: serine) following the "split-couple-recombine" method [18-20]. The selected peptides 8mer peptides ANAKIKKK-GSG, FEKWAKAH-GSG, FSHHSWKF-GSG, KAWFKHWN-GSG, KHSKAIAA-GSG, KWKHSHKW-GSG, WHAKKSHF-GSG, WHAKKSKF-GSG, and the 6-mer peptides AAHFHK-GSG, KHAWIF-GSG, KFHAWN-GSG, NHNKIH-G, and SHWHWA-GSG were synthesized on Toyopearl AF-Amino-650 M resin at the density of \sim 0.15 mmol of peptide per gram of resin. Following chain elongation, the peptides were deprotected via acidolysis using a cleavage cocktail containing TFA, thioanisole, anisole, and EDT (94/3/2/1) for 2 hrs. Following deprotection, the ChemMatrix library resins were rinsed with DCM and DMF and stored in DMF at 4 °C, whereas the peptide-Toyopearl resins were washed sequentially with DCM, DMF, methanol, and stored in 20% v/v aqueous methanol.

2.3. Fluorescent labeling of AAT and CHO HCPs

The AAT and the host cell proteins (HCPs) contained in the CHO cell culture harvest were labeled using NHS-Alexafluor 594 (NHS-AF594, red) and NHS-Alexafluor 488 (NHS-AF488, green), respectively. Both dves were initially dissolved in anhydrous DMSO to a concentration of 10 mg/mL. A volume of 1 µL of NHS-AF594 was slowly added to 100 µL of AAT solution at 2 mg/mL in PBS pH 7.4, while 200 µL of NHS-AF488 was added to 4 mL of null CHO-S cell culture fluid at 1.0 mg/mL total HCP concentration. The labeling reactions were allowed to proceed for 1 hr at room temperature, under dark and gentle agitation. The unreacted dyes were removed using 0.5 mL ZebaTM Dye and Biotin Removal Spin Columns (ThermoFisher Scientific, Waltham, MA). The concentration of the labeled proteins in solution was determined by Bradford assay. The absorbance of the solutions of AF488-labeled CHO HCPs and AF594-labeled AAT was measured by UV spectrophotometry at the wavelength of 490 and 590 nm, respectively, using a Synergy H1 plate reader (Biotek, Winooski, VT).

2.4. Dual-Fluorescence screening of peptide library against AAT in CHO cell culture fluid

A screening mix was initially prepared by spiking AF594-labeled AAT in AF488-labeled CHO cell culture fluid to obtain a

final concentration of 1.0 mg/mL for AAT and 0.5 mg/mL for CHO host cell proteins. Aliquots of 10 μ L of library beads were initially equilibrated with PBS at pH 7.4 and subsequently incubated with 40 μ L of screening mix for 2 hrs at room temperature in dark. The beads were thoroughly washed with PBS at pH 7.4 and 0.1% v/v Tween 20 in PBS at pH 7.4 and sorted automatically using the microfluidic screening device developed in prior work [14,17,21]. Beads displaying strong red-only fluorescence were selected, individually incubated with 100 μ L of 0.1 M glycine buffer pH 2.5 for 1 hr at room temperature and in the dark to elute the bound AF594-labeled AAT, and rinsed with MilliQ water and acetonitrile. The beads were finally analyzed via Edman degradation using a PPSQ-33A protein sequence (Shimadzu, Kyoto, Japan) to sequence the selected peptides.

2.5. Static binding capacity and affinity of peptide-Toyopearl resins

The selected sequences were synthesized on Toyopearl AF-Amino 650 M resin as described in Section 2.2 and evaluated via isotherm binding studies of AAT in non-competitive mode (i.e., pure AAT in PBS at pH 7.4) as described in prior work [14,22,23]. Aliquots of 50 µL of peptide-Toyopearl resin were transferred in a tube, swollen in 20% v/v aqueous methanol, washed in MilliQ water, and finally equilibrated in PBS at pH 7.4. The resin aliquots were individually incubated with 0.5 mL of a solution of AAT at different concentrations (0.1, 0.25, 0.5, 0.75, 1.0, 1.5, 2.0, and 5.0 mg/mL) for 1.5 hrs at room temperature under gentle rotation. After incubation, the resin aliquots were centrifuged and the supernatants collected as unbound (UB) fraction; the resins were also washed with 0.5 mL of PBS for 30 min, and the supernatants were combined with the corresponding UB fractions. These were finally analyzed by Micro BCA Protein Assay kit to determine the concentration C* of unbound AAT in solution at the equilibrium with the resin, from which the amount q of bound AAT per volume of resin was determined by mass balance. The values of q vs. C^* were plotted and fit using a Langmuir isotherm (Eq. (1)) to determine the values of maximum binding capacity (Q_{max}) and affinity dissociation constant (K_D) .

$$q = \frac{Q_{max} \cdot C^*}{K_D + C^*} \tag{1}$$

2.6. Dynamic binding capacity of peptide Toyopearl resins

The dynamic binding capacity at 10% breakthrough (DBC_{10%}, mg of AAT per mL resin) of the selected peptide-Toyopearl resins and the control AAT Select resin was measured as reported in prior studies [24-26]. A volume of 0.1 mL of resin was wet packed in a Vici Jour PEEK column, washed with 10 column volumes (CVs) of 20% v/v ethanol, deionized water (3 CVs), and finally equilibrated with 10 CVs of binding buffer. The binding buffers used in this study were (i) 0.15 M NaCl in 20 mM Bis-Tris-HCl buffer at pH 6.0, (ii) PBS buffer at pH 7.4, and (iii and iv) 0.15 M NaCl in 50 mM Tris-HCl buffer at pH 7.4 or pH 8.0. A volume of 2 mL of solution of human AAT at 1 mg/mL in PBS buffer was continuously loaded on the column at the flow rate of either 0.05 mL/min (residence time, RT: 2 min) or 0.02 mL/min (RT: 5 min). After loading, the resin was washed with 10 CVs of binding buffer at the flow rate of 0.1 mL/min. AAT elution was then performed with 20 CVs of PBS in 2 M MgCl₂ at pH 7.4 at the flow rate of 0.2 mL/min. The resin was regenerated with 10 CVs of glycine buffer at pH 2.0 at the flow rate of 0.2 mL/min. The effluents were continuously monitored by UV spectrometry at 280 nm and the resulting chromatograms were utilized to calculate the DBC_{10%} of AAT.

Table 1HPLC method for AAT quantification via analytical affinity chromatography using AAT Select resin.

Time (min)	Flowrate (mL/min)	PBS pH 7.4	0.1 M Glycine buffer, pH 2.5
0.00	0.5	100%	0%
2.00	0.5	100%	0%
2.01	0.5	0%	100%
6.00	0.5	0%	100%
6.01	0.5	100%	0%
10.00	0.5	100%	0%

2.7. Purification of AAT from CHO cell culture supernatant using peptide-Toyopearl resins

Each peptide-functionalized resin was individually wet packed in the 0.5 mL Alltech PEEK column, washed with 20% v/v ethanol (10 CVs) and deionized water (3 CVs), and equilibrated with 10 CVs of PBS at pH 7.4. A volume of 2.5 mL of AAT at \sim 1 mg/mL in CHO-S cell culture supernatant (HCP titer ~ 0.35 mg/mL) was loaded on the column at the flow rate of 0.25 mL/min (RT: 2 min). After loading, the resin was washed with binding buffer (5 CVs) to recover the UV_{280nm} baseline. AAT elution was then performed using 15 CVs of PBS solution with 2 M MgCl2 at pH 7.4 at the flow rate of 0.5 mL/min. The resin was regenerated with 10 CVs of glycine buffer at pH 2.0 at the flow rate of 0.5 mL/min. The collected flow-through and elution fractions were analyzed by analytical HPLC (see Section 2.8) to measure the AAT concentration and determine the values of product yield, and size exclusion chromatography (SEC-HPLC, see Section 2.9) and gel electrophoresis (see Section 2.10) to determine the values of product purity.

2.8. Quantification of AAT yield

The AAT titer in the chromatographic fractions were measured via analytical affinity chromatography using an AAT Select column installed on a Waters Alliance 2690 separations module system with a Waters 2487 dual absorbance detector (Waters Corporation, Milford, MA, USA). The AAT Select resin was wet packed in a Vici Jour PEEK 2.1 mm ID x 30 mm column (0.1 mL) and initially equilibrated with PBS buffer at pH 7.4. A volume of 50 μL of each sample or standard was loaded on the column and processed using the analytical method proceeded outlined in Table 1. The effluent was monitored by 280 nm absorbance (A280), and the AAT concentration was determined based on the area of the elution peak; pure AAT at 0.1, 0.2, 0.4, 0.6, 0.8, 1.0, and 2.0 mg/mL was utilized to construct the standard curve.

The values of yield (Y,%) and binding capacity (Q, mg of AAT per mL resin) of AAT product were calculated using Eqs. (2) and (3), respectively.

$$Y = \frac{C_{AAT,El} \times V_{El}}{C_{AAT,L} \times V_{L}} \times 100\% \tag{2}$$

$$Q = \frac{C_{AAT,L} \times V_L - C_{AAT,FT} \times V_{FT}}{V_R}$$
 (3)

Wherein $C_{AAT,FT}$, $C_{AAT,EI}$, and $C_{AAT,L}$ are the AAT concentration in the flow-through and elution fractions, and in the load, respectively; V_{FT} , V_{EI} and V_{L} are the volume of the flow-through and elution fractions and the load, respectively; and V_{R} is the volume of resin.

2.9. Quantification of AAT purity by size-exclusion chromatography (SEC)

The collected fractions were also analyzed by analytical SEC using a BioResolve SEC mAb Column, 200 Å, 2.5 μ m, 7.8 \times 300 mm

column (Waters, Milford, MA) operated with a 40-min isocratic method using PBS at pH 7.4 as mobile phase. A volume of 20 μ L of sample was injected and the effluent continuously monitored by UV spectrometry at 280 nm absorbance (A280). The purity of AAT (P,%) was calculated using Eq. (4).

$$P = \frac{A_{AAT,EI}}{A_{AAT,EI} + A_{HCP,EI}} \times 100\%$$
 (4)

Wherein $A_{AAT,EI}$ and $A_{HCP,EI}$ are the values of area of the peaks respectively related to AAT and CHO host cell proteins (based on the residence time of the peak) recorded in the SEC analysis of the elution fractions generated as described in Section 2.7.

2.10. Quantification of AAT purity by sodium dodecyl sulfate polyacrylamide gel electrophoresis (SDS-PAGE)

The collected fractions were analyzed by reducing SDS-PAGE using 4–20% Mini-PROTEANTM TGXTM Precast protein gels (Bio-Rad, Hercules, CA) with Tris/Glycine/SDS buffer as running buffer. The fractions were diluted or concentrated to a total protein concentration of $\sim\!0.5$ mg/mL and a volume of 2 μ L of different samples were loaded to the wells of SDS-PAGE gels. The sample stripes were concentrated under 80 V for about 30 min and separated under 120 V for about 1 hr. Then the gels were stained by a SilverQuestTM Silver Staining Kit (ThermoFisher, Waltham, MA). Finally, the stained protein stripes were imagined by the Gel Doc2000 imaging system (Bio-Rad).

2.11. In silico evaluation of AAT binding pockets and AAT:peptide complexes

The homology structure of human AAT was initially prepared using Protein Prep Wizard (PPW, Schrödinger, New York, NY) [27] by correcting missing atoms and/or side chains (PRIME), removing salts and ligands, adding explicit hydrogens, and optimizing the hydrogen-bonding network on PDB IDs 1HP7, 5IO1, and 4PYW; the ionization state at pH 7.4 and minimization of the protein structure were finally performed using PROPKA [28,29]. The adjusted structure was then analyzed using SiteMap to identify sites for ACP binding [30–32], and the sites with high S-score (>0.8) and D-score (>0.9) were selected for ACP docking.

Peptides ANAKIKKK-GSG, FEKWAKAH-GSG, FSHHSWKF-GSG, KAWFKHWN-GSG, KHSKAIAA-GSG, KWKHSHKW-GSG, WHAKKSHF-GSG, WHAKKSKF-GSG, AAHFHK-GSG, KHAWIF-GSG, KFHAWN-GSG, NHNKIH-G, and SHWHWA-GSG were constructed using the molecular editor Avogadro. The equilibration and production steps were performed in AMBER using the Amber ff19SB force field [33]. Briefly, every peptide was placed in a simulation box with periodic boundary and containing 1000 water molecules (TIP3P model), and equilibrated with 10,000 steps of steepest gradient descent; the ACP was then heated to 300 K in an NVT ensemble for 250 ps with 1 fs time steps, and equilibrated to 1 atm with a 500-ps NPT simulation with 2 fs time steps. The production runs were performed in the NPT ensemble at T = 300 K and P = 1 atm using the Nosé-Hoover thermostat and the Parrinello-Rahman barostat, respectively [34,35]. The leap-frog algorithm was used to integrate the equations of motion, with integration steps of 2 fs, and the atomic coordinates were saved every 2 ps. All covalent bonds were constrained using the LINCS algorithm, the short-range electrostatic and Lennard-Jones interactions were calculated using cut-off values of 1.0 nm and 1.4 nm, and the particle-mesh Ewald method was utilized for long-range electrostatic interactions [36]; the list of non-bonded interactions was updated every 5 fs using a cutoff of 1.4 nm.

Finally, the peptides were docked in silico against the putative binding sites on human AAT using the docking software

HADDOCK (High Ambiguity Driven Protein-Protein Docking, v.2.4) [37,38]. The residues on the selected binding sites of AAT and the X_1 - $X_{6/8}$ residues on the peptides were marked as "active", and the surrounding residues were marked as "passive". The docked AAT:peptide structures were grouped in clusters of up to 20 complexes based on $C\alpha$ RMSD and ranked using the dMM-PBSA score [39]. Finally, the top AAT:peptide complexes were refined via 100-ns atomistic MD simulations and evaluated to estimate the free energy of binding (Δ GB).

3. Results and discussion

3.1. Tailoring a peptide library focused to the discovery of AAT-binding peptides

The core secondary structure of α -1 antitrypsin (AAT, \sim 54 kDa, pI \sim 4.8) comprises nine α -helices (A - I) and three β -pleated sheets (A - C, Fig. S1A) [40-42]. The reactive center loop (RCL) of AAT, which bridges strand 5 of β -sheet A (s5A) to strand 5 of β -sheet C (s1C) and arches away from this core structure [12], features an inhibitory activity against neutrophil elastase, which protect tissues from enzymatic attack and inflammation [43,44]. The inhibitory mechanism of AAT is initiated by the interaction between the RCL and the active site of neutrophil elastases. Depending on their sequence and orientation, these enzymes cleave dipeptide sequence P1-P1' in the RCL region, resulting in a Michaelistype complex between AAT and the elastase, which blocks the latter from triggering inflammatory effects [45,46]. As an active site, the RCL and its surrounding domains (β -pleated sheets B and C, and α -helices G and H) are not suitable targets for peptide ligands, since the formation and dissociation of affinity complexes with ligands may cause structural and biochemical alterations, leading to unwanted loss of binding specificity and inhibitory activity towards target elastases. Notably, α -helices A – E of the core AAT structure are removed from the RCL region and represent an ideal target site for AAT capture.

We therefore performed an in silico "druggability" study of the core AAT structure PDB IDs: 1HP7, 5IO1, 4PYW using SiteMap [30-32] and identified 5 putative epitope with appropriate morphological features - namely, pocket depth (PD), solvent-accessible surface area (SASA), and pocket volume (PV)) and biophysical properties (i.e., isoelectric point (pI), polarity, and grand average hydropathy (GRAVY) index) to harbor peptide ligands [47]. The structure and properties of the identified epitopes are reported in Figure S1B and Table S1, respectively. Four of the five epitopes are situated in the core structure of AAT and were therefore utilized to guide the design of a focused library of peptides; the fifth epitope overlapped with the reactive loop of AAT and was therefore excluded from targeted design. Notably, the four target binding sites feature a similar pocket depth (12.7 - 14.1 Å) and volume (1180 -1600 Å3) as well as distinct negative electrostatic (pI \sim 3.7 – 5.2) and amphiphilic (GRAVY index ~ -0.05 to -0.65) character. These properties recommend the use of small peptides (max. 10 amino acids, [48]) rich in cationic, polar, and aromatic residues. Accordingly, we resolved to construct two libraries of linear peptides: (i) the peptide length was set at 6 and 8 residues, which balance the requirements of binding strength and selectivity with the considerations of cost and scalability [49-52]; (ii) the combinatorial positions were randomized using amino acids capable of forming a network of non-covalent interactions with the target binding pockets, namely cationic residues histidine and lysine (H and K), polar residues asparagine, serine, and glutamate (N, S, and E), aromatic residues phenylalanine and tryptophan (F and W), and alanine (A) serving as a semi-rigid amino acid spacer; (iii) a GSG (Gly-Ser-Gly) tripeptide spacer was introduced between the combinatorial segment of the library and the resin to promote the display of the

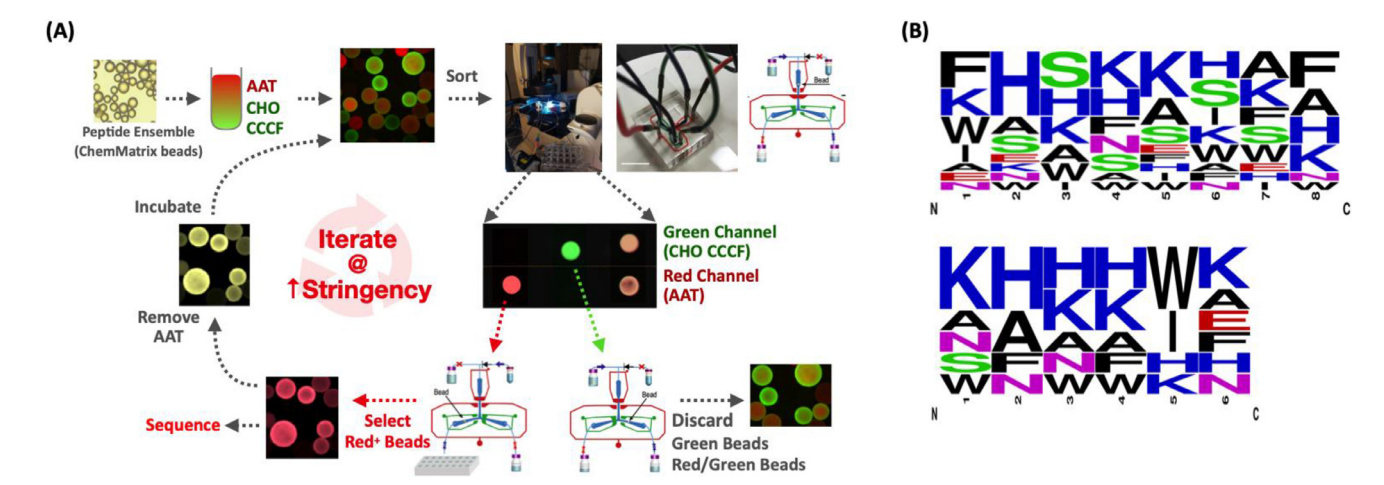


Fig. 1. Identification of AAT-binding peptides. (A) A library of peptide-ChemMatrix beads was (1) incubated with a screening feed comprising AF594-labeled AAT and AF488-labeled CHO host cell proteins, washed, and (2) fed to the bead-sorting microfluidic device; (3) green-only and red-and-green beads were discarded, whereas the red-only beads were selected as positive; (4) the selected beads were regenerated and re-entered into the screening loop; (5) finally, the positive beads were analyzed by Edman degradation to identify candidate AAT-binding sequences. (B) Sequence homology of selected 8-mer and 6-mer peptides.

variable segment of the peptides, which improves the efficiency of both library screening and Edman sequencing. The peptide libraries were synthesized on ChemMatrix beads via Fmoc/tBu-based chemistry following the "split-couple-and-recombine" technique [53,54]. ChemMatrix has been extensively utilized as a substrate for ligand selection by our group [13,14,55]: these porous, hydrophilic, translucent microparticles (pore diameter >100 nm, particle diameter ~200 – $250~\mu m)$ proved an excellent substrate for the synthesis and selection of candidate peptide ligands for chromatographic applications.

3.2. Combinatorial selection of peptide ligands against human AAT

In prior work our team developed a device for automating the rapid selection of peptide ligands targeting biological targets [14,21]. The device sorts beads from solid-phase peptide libraries and provides (i) simultaneous positive and negative selection by dual fluorescent labeling to isolate peptides with high binding affinity and selectivity and (ii) rapid screening at a rate of ~350 beads per hr. The device comprises a microfluidic bead-sorting chamber, a multiple wavelength fluorescent microscope, and software for real-time bead monitoring, image processing, and screening (Fig. 1A). The software performs rapid acquisition of fluorescent bead images and image analysis and instructs the sorting of a bead to either a selection receptacle or to waste. We utilized this beadsorting device to screen the peptide library against a screening mix containing AAT labeled with red AlexaFluor 594 (AF594) spiked in a mixture of Chinese hamster ovary host cell proteins (CHO HCPs) collectively labeled with green AlexaFluor 488 (AF488). Library beads featuring a strong red-only fluorescence (high AATbinding affinity and selectivity) were selected and analyzed by Edman degradation to identify the peptide sequences displayed thereon. The resultant ensemble of 13 candidate ligands (five 5mer and eight 8-mer sequences) are listed in Table S2; the homology analysis of the sequences is reported in Fig. 1B.

3.3. Evaluation of AAT-binding peptides via in vitro and in silico AAT binding studies

The selected peptides were synthesized on Toyopearl AF-Amino 650 M resin via Fmoc/tBu synthesis and tested via static binding studies in non-competitive conditions (i.e., pure AAT in PBS at pH 7.4). Toyopearl resin was selected for ligand conjunction owing

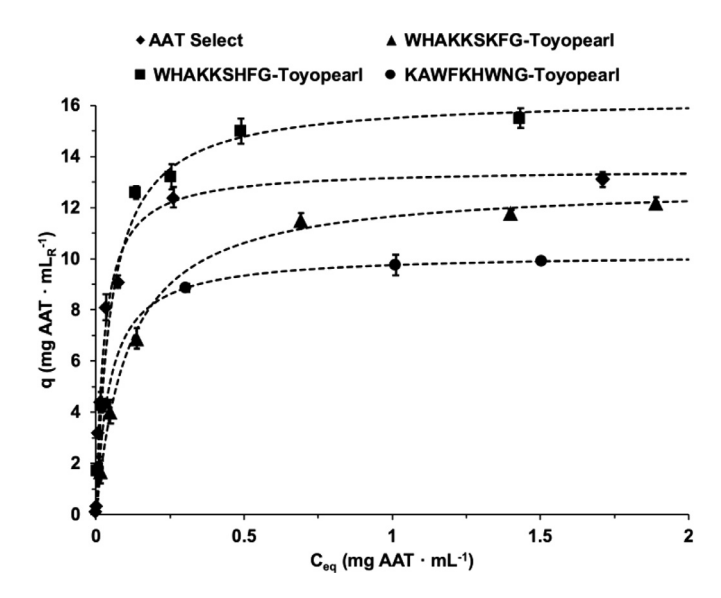


Fig. 2. Adsorption isotherms of AAT on selected peptide-Toyopearl adsorbents and reference AAT Select resin.

to its high chemical and mechanical stability as well as low nonspecific protein adsorption, which make it an ideal substrate for direct peptide conjugation and protein chromatography [22,56,57]. The AAT adsorption isotherms of ANAKIKKKG-, FEKWAKAHG-, FSHHSWKFG-, KAWFKHWNG-, KHSKAIAAG-, KWKHSHKWG-, WHAKKSHFG-, WHAKKSKFG-, AAHFHKG-, KHAWIFG-, KFHAWNG-, NHNKIHG-, and SHWHWAG-Toyopearl resins were constructed to rank the candidate peptide ligands based on the values of maximum binding capacity ($Q_{max} \sim \text{mg}$ of AAT per mL of resin) and affinity (i.e., dissociation constant, $K_D \sim \mu M$) of the corresponding adsorbents. To this end, the adsorption data measured with the above-listed adsorbents across an ample range of AAT concentration (0.1 - 5 mg/mL) were fit against Langmuir isotherms (Fig. 2) and the resulting fitting parameters Q_{max} and K_D are reported in Table 2. Notably, all adsorption plots fit the Langmuir isotherm well, returning values of K_D comprised within 0.35 and 6.9 μ M, thus indicating that the peptides bind AAT via true affinity interaction. The values of Q_{max} , however, fluctuated within a rather large interval, ranging from a minimum of 3.5 mg/mL, unacceptable for bioprocessing, to a maximum of 16.3 mg/mL, in line with that of AAT Select resin.

Table 2Values of AAT maximum binding capacity (Q_{max}) and dissociation constant (K_D) of peptide-Toyopearl resins obtained by fitting the adsorption data in Fig. 2 using the Langmuir isotherm equation.

Adsorbent	Q_{max} (mgAAT per mLR)	K_D (μ M)	Adsorbent	Q_{max} (mgAAT per mLR)	K_D (μ M)
ANAKIKKKG-Toyopearl	3.5	6.70	WHAKKSKFG-Toyopearl	12.9	2.09
FEKWAKAHG-Toyopearl	5.1	4.67	AAHFHKG-Toyopearl	8.7	4.71
FSHHSWKFG-Toyopearl	9.4	3.63	KHAWIFG-Toyopearl	7.2	1.42
KAWFKHWNG-Toyopearl	10.2	0.87	KFHAWNG-Toyopearl	8.9	2.48
KHSKAIAAG-Toyopearl	9.1	3.62	NHNKIHG-Toyopearl	6.3	2.32
KWKHSHKWG-Toyopearl	15.8	0.63	SHWHWAG-Toyopearl	7.0	3.28
WHAKKSHFG-Toyopearl	16.3	0.95	AAT Select	13.5	0.51

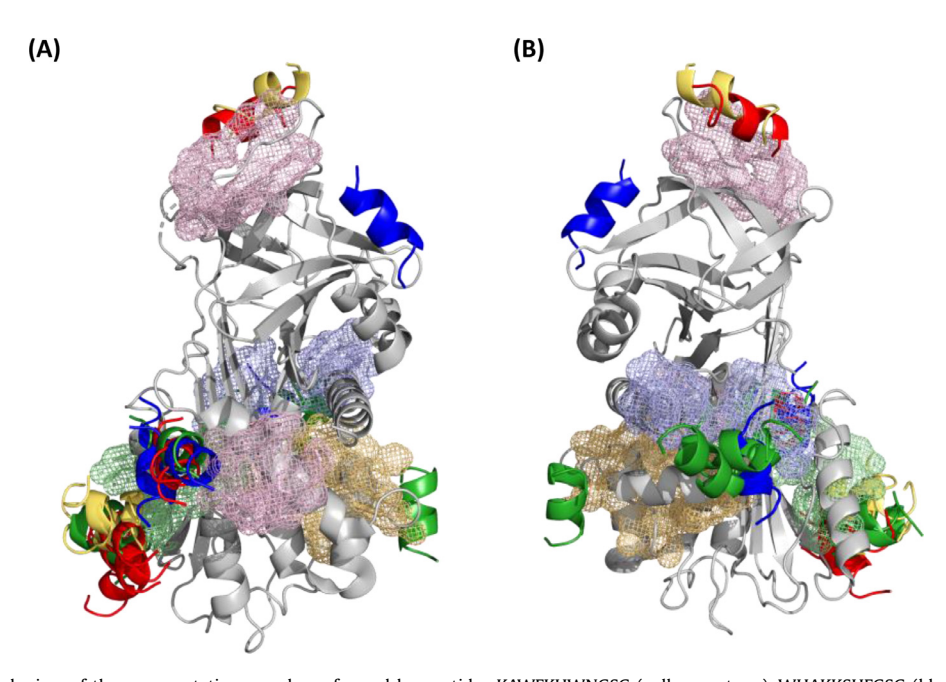


Fig. 3. (A) front and (B) back view of the representative complexes formed by peptides KAWFKHWNGSG (yellow cartoon), WHAKKSHFGSG (blue cartoon), KWKHSHKWGSG (red cartoon), and WHAKKSKFGSG (green cartoon) with human AAT (PDB ID: 1HP7, 5IO1, 4PYW; gray cartoon) obtained via molecular docking and dynamics simulations; the targeted binding sites are red, blue, green, and orange mesh.

To gather a molecular-level understanding of the differences in binding strength among the various peptides, we evaluated the sequences that featured the highest (WHAKKSKF-GSG, WHAKKSHF-GSG, KWKHSHKW-GSG, FSHHSWKF-GSG, and KHAWIF-GSG) and lowest (AAHFHK-GSG, KHSKAIAA-GSG, FEKWAKAH-GSG, and ANAKIKKK-GSG) binding performance via molecular docking and dynamics analysis. The secondary structure of the peptides, obtained via MD simulations in explicit solvent, were docked against the homology structure of AAT obtained from published structures (PDB IDs: 1HP7, 5IO1, 4PYW). Docking was conducted in HADDOCK v. 2.4 [37,38] and was focused on the putative binding sites obtained from an initial "druggability" study (Figure S1B). Following a method developed in prior work [14,15,58], we imposed the -GSG tripeptide appended on the C-terminal end of the peptides not to bind AAT: constraining the degrees of orientational freedom of the peptides mimics their conjugation onto the surface of the chromatographic resin, and has been consistently found to return values of K_D , in silico that match the corresponding values of K_D , in vitro more accurately than those obtained with full orientational freedom [59]. The resulting complexes were refined via 100-ns MD simulations in explicit solvent to obtain values of binding free energy (Δ Gb) and calculate the corresponding K_D , in silico. The resulting complexes are reported for each peptide sequence in Figure S2, while notable results are collated in Fig. 3; the resultant values of K_D , in silico are reported in Table 3 for each AAT site: peptide pair. Upon close examination of these results, we drew four main conclusions. Firstly, the values of K_D , in silico align well with the

Table 3 Values of binding affinity (K_D ,in-silico) of the complexes formed by selected peptides with human AAT (PDB ID: 1HP7, 5IO1, 4PYW) obtained via molecular docking and dynamics simulations. The binding affinity of the complexes formed by AAT and antibodies were calculated by analyzing the PDB IDs 6HX4 and 6I3Z.

Adsorbent	K_D ,in silico (M)	Adsorbent	K_D ,in silico (M)
AAHFHK-GSG	8.2 · 10 ⁻⁶	WFNHKSKG-GSG	1.2 · 10-6
ANAKIKKK-GSG	$2.3 \cdot 10^{-5}$	WHAKKSHF-GSG	$8.8 \cdot 10^{-7}$
FEKWAKAH-GSG	$7.1 \cdot 10^{-6}$	WHAKKSKF-GSG	$1.8 \cdot 10^{-6}$
FSHHSWKF-GSG	$6.1 \cdot 10^{-6}$	KFHAWN-GSG	$7.8 \cdot 10^{-6}$
KAWFKHWN-GSG	$3.0 \cdot 10^{-6}$	KHAWIF-GSG	$3.9 \cdot 10^{-6}$
KHSKAIAA-GSG	$9.3 \cdot 10^{-7}$	Fab1 (PDB ID: 6HX4)	$7.9 \ 10^{-6}$
KWKHSHKW-GSG	$3.6 \cdot 10^{-6}$	Fab2 (PDB ID: 6I3Z)	$1.5 \ 10^{-10}$

values of K_D ,in vitro, which is attributed to the directionality of peptide docking on AAT, thus confirming the ranking of the candidate ligands obtained from the binding isotherm studies; notably, the sequences featuring the lowest values of K_D ,in vitro (highest affinity) were found to target neighboring binding sites on the AAT surface, suggesting that contiguous peptides on the surface of the resin may interact with one AAT molecule to form a multipoint interaction (a mechanism known as avidity, [60,61]). Secondly, most of the tested sequences indeed targeted the binding pockets localized in the core of AAT, indicating that the design of the library based on the initial druggability studies was conducted successfully; sequences KAWFKHWNG and KWKHSHKWG, which bound the active loop, as well as ANAKIKKKG, FEKWAKAHG, and

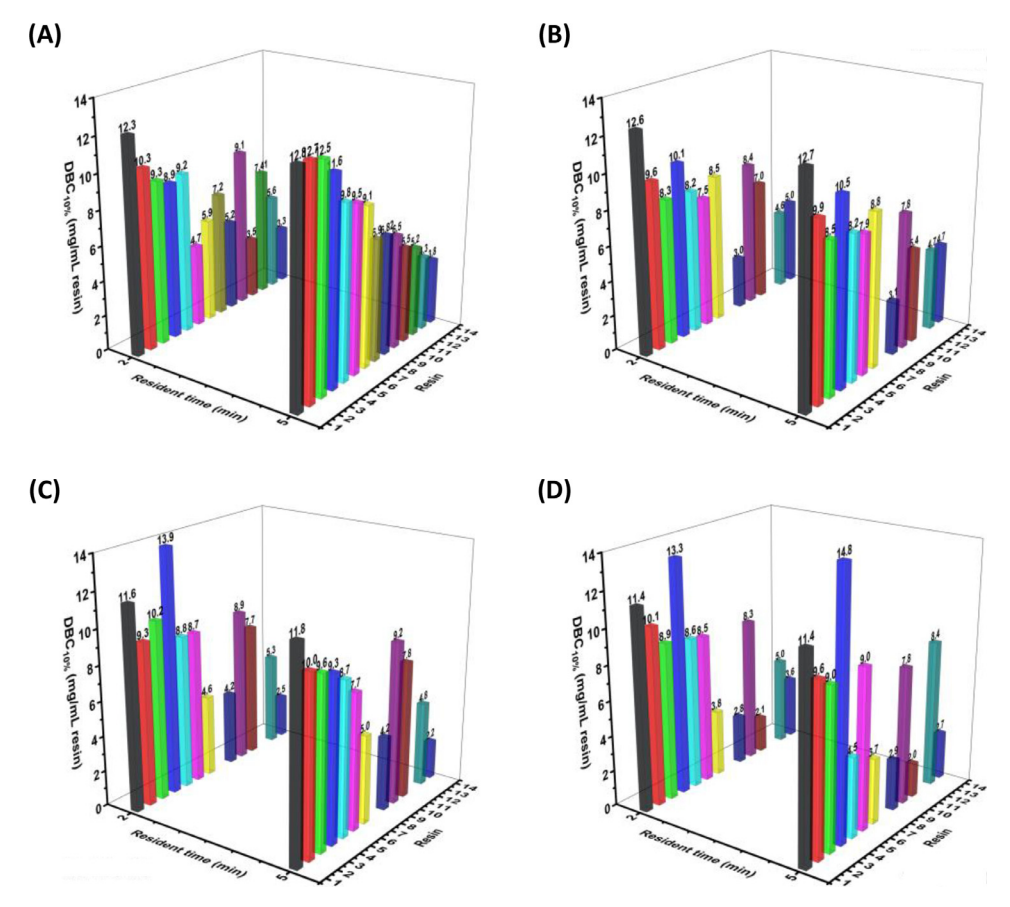


Fig. 4. Values of dynamic binding capacity of 10% AAT flow-through (*DBC*_{10%}, mg of AAT per mL resin) measured at two values of residence time (RT: 2 and 5 min) and four different buffer compositions and pHs, namely (A) PBS at 7.4, (B) 50 mM Tris- HCl at 7.4, (C) 20 mM Bis-Tris- HCl at 6.0, and (D) 50 mM Tris- HCl at pH 8.0); Resin 1: Alpha-1 antitrypsin Select; Resin 2: WHAKKSKFG-Toyopearl; Resin 3: WHAKKSHFG-Toyopearl; Resin 4: KWKHSHKWG-Toyopearl; Resin 5: FSHHSWKFG-Toyopearl; Resin 6: KAWFKHWNG-Toyopearl; Resin 7: AAHFHKG-Toyopearl; Resin 8: KFNHWNG-Toyopearl; Resin 9: KHSKAlAAG-Toyopearl; Resin 10: KHAWIFG-Toyopearl; Resin 11: SHWHWAG-Toyopearl; Resin 12: NHNKIHG-Toyopearl; Resin 13: FEKWAKAHG-Toyopearl; Resin 14: ANAKIKKKG-Toyopearl.

AAHFHKG, which bound with insufficient affinity, were discarded. Thirdly, the peptides with the highest number of putative binding sites on AAT – irrespective of their mutual position on the surface of the protein – afforded the highest binding capacity; this suggests that the ligands with more versatile AAT binding achieve a better protein coverage of the resin's surface, since proteins can be effectively adsorbed and retained in multiple spatial orientations, resulting in higher capacity. Fourthly, the putative binding sites of all the peptide ligands evaluated in this work are not involved in N-glycosylation (based on PDB IDs 7API, 8API, and 9API, Figure S2); this result was corroborated by the AAT purification studies discussed below.

3.4. Evaluation of AAT-binding peptides via dynamic binding measurements

Following the equilibrium binding studies, the selected peptide-Toyopearl resins were evaluated under dynamic conditions to evaluate the interplay of kinetic factors – chiefly, the AAT transport within the chromatographic particles and the formation of AAT:peptide complexes – on the resultant binding capacity. To that end, the dynamic binding capacity at 10% breakthrough ($DBC_{10\%}$, mg of AAT per mL of resin) of the peptide-Toyopearl resins was measured at two values of residence time (RT), namely 2 and 5 min, and four different buffer compositions, namely 20 mM Bis-Tris-HCl buffer (0.15 M NaCl) at pH 6.0, PBS buffer at pH 7.4, and 50 mM Tris-HCl buffer (0.15 M NaCl) at pH 7.4 and 8.0, and compared with that of AAT Select from Cytiva (Fig. 4; the corresponding breakthrough curves are reported in Figure S3).

When measured in PBS at pH 7.4, the values of DBC10% (RT of 5 min) of the top three peptide-Toyopearl resins were found to compare well with the control affinity adsorbent, AAT Select resin (12.8 mg/mL): specifically, WHAKKSKFG-, WHAKKSHFG-, and KWKHSHKWG-Toyopearl resins featured 12.7 mg/mL, 12.5 mg/mL, and 11.6 mg/mL, respectively (Fig. 4A). Notably, these values of dynamic capacity and their equilibrium counterparts (Q_{max} , Table 2) were nearly identical for AAT Select and WHAKKSKFG-Toyopearl resins, while they differed for WHAKKSHFG- and KWKHSHKWG-Toyopearl resins. Furthermore, when the RT was lowered to 2 min, the DBC10% of AAT Select resin decreased only slightly to 12.3 mg/mL, whereas WHAKKSKFG-, WHAKKSHFG-, and KWKHSHKWG-Toyopearl resins presented a more substantial loss $(\sim 20\%)$ down to 10.3, 9.3, and 8.9 mg/mL, respectively. These results indicate that, as it is commonly observed, the mass transfer kinetics is a key determinant of binding capacity. Different variations in DBC_{10%} with feed flow rate are also expected given the different morphology of the beads: AAT Select is an agarose-based gel featuring an "open cell" porosity, whereas the peptide-Toyopearl adsorbents are polymethacrylate-based resin with channel-like pores; accordingly, the binding capacity of Toyopearl-based adsorbents may present a stronger dependence upon residence time (i.e., flowrate during adsorption) compared to AAT Select resin.

When measured in Tris buffer at comparable conductivity (\sim 15 mS/cm) and pH of 7.4, however, the values of $DBC_{10\%}$ did not show any appreciable variation with the feed flowrate: whether evaluated at the RT of 2 or 5 min, AAT Select maintained a binding capacity \sim 12 mg/mL, while WHAKKSKFG- and WHAKKSHFG-Toyopearl resins maintained values averaging at 9.7

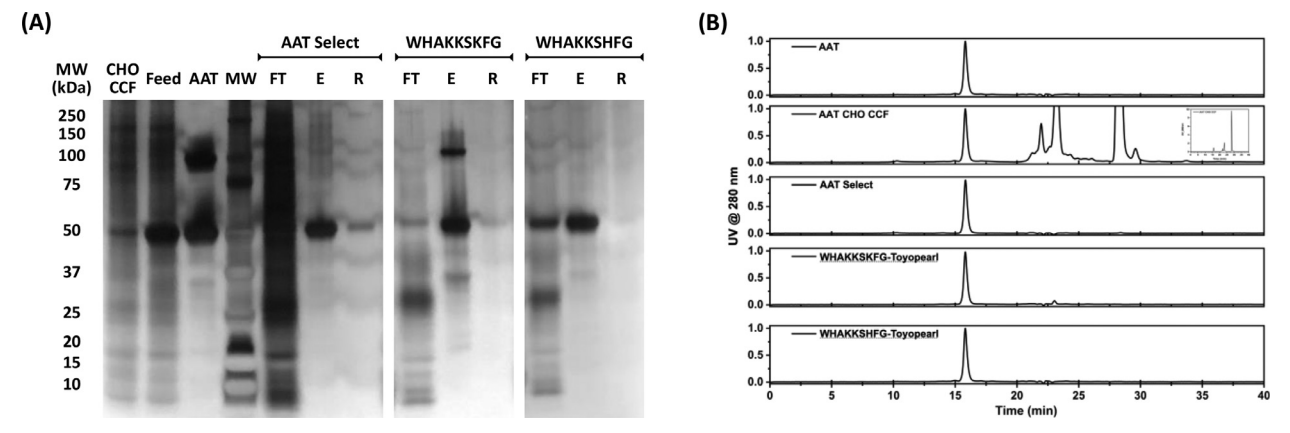


Fig. 5. (A) SDS-PAGE analysis (reducing condition, silver staining) of the chromatographic fractions obtained by purifying AAT from CHO cell culture fluids using AAT Select, WHAKKSKFG-Toyopearl and WHAKKSHFG-Toyopearl resins. Labels: MW, molecular weight marker; AAT, alpha-1 antitrypsin standard; Feed, feedstock (AAT titer: 1.15 mg/mL; HCP titer: 0.5 mg/mL); FT, flow-through fraction; E, eluted fraction in 2 M MgCl₂ in PBS at pH7.4; R, regeneration fraction in 0.1 M glycine at pH 2.5. (B) SEC analysis of pure AAT, AAT spiked in CHO-S CCF, and AAT purified using AAT Select, WHAKKSKFG-Toyopearl and WHAKKSHFG-Toyopearl resins.

and 9.3 mg/mL. The sole exception in this trend was represented by KWKHSHKWG-Toyopearl resin, whose binding capacity in Tris buffer was significantly higher than its counterpart in PBS, especially at pH 6.0 and 8.0, reaching the highest value registered in this study (14.8 mg/mL).

To elucidate these phenomena, we resolved to conduct additional molecular docking and dynamics simulations of AAT:WHAKKSKFG, AAT:WHAKKSHFG, and AAT:KWKHSHKWG binding in presence of Tris at pH 6.0, 7.0, and 8.0. At pH 7.0, Tris molecules adsorb onto the aspartate/glutamate-rich sites on the surface of AAT, thus mitigating its anionic character (the pI of AAT is 4.2 – 4.6, [62]). We hypothesize that Tris complexation promotes AAT binding by minimizing the electrostatic repulsion between incoming AAT molecules and those already adsorbed on the pore surface (Figure S4A). Furthermore, Tris molecules do not interfere with AAT:peptide interactions, because either they do not adsorb at the peptide-binding sites or adsorb weakly and are easily displaced by the peptide ligands (Figure S4B).

Regarding ligand KWKHSHKWG, lowering the pH from 7.0 to 6.0 increases the positive charge of its two histidine (H) residues, resulting in a stronger interaction with AAT and an additional binding pose (i.e., a cluster of AAT:KWKHSHKWG complexes with C_{α} RMSD < 7.5 Å, Figure S4C). Conversely, increasing the pH to 7.0 to 8.0 strengthens the contribution of the electrostatic interaction within the AAT:KWKHSHKWG complexes: the anionic character of the AAT surface in correspondence of the putative binding sites increases with pH, thus promoting KWKHSHKWG binding (Figure S4D and S4E).

Collectively, these in silico findings provide rationale to otherwise counterintuitive measurements of $DBC_{10\%}$ obtained at different values of residence time and properties of the mobile phase. By offering a valuable insight into the balance between the kinetics of mass transfer and AAT:peptide biorecognition, these results can be leveraged to optimize the chromatographic operation.

Having assigned a threshold of binding capacity at 10 mg/mL to ensure feasibility of the adsorbent in a AAT purification process, the adsorbents WHAKKSHFG-, WHAKKSKFG-, and KAWFKHWNG-Toyopearl resins were selected for AAT purification from a CHO cell culture harvest.

3.5. Purification of AAT from CHO cell culture harvests using AAT-binding adsorbents

Performing the library screening under competitive conditions, i.e., using a screening mix that combines AAT and CHO HCPs at a

Values of product yield and purity obtained by purifying AAT from CHO cell culture fluids using AAT Select and peptide-Toyopearl resins.

Adsorbent	Yield	Purity
WHAKKSHFG-Toyopearl	75.0%	96.8%
WHAKKSKFG-Toyopearl	76.6%	93.1%
KAWFKHWNG-Toyopearl	51.2%	89.1%
AAT Select	79.0%	96.1%

ratio that mimics industrial recombinant fluids, has been designed to afford candidate peptide ligands with selective biorecognition to ensure their ability to isolate AAT from complex sources in bind-and-elute mode. Adsorbents WHAKKSKFG- and WHAKKSHFG-Toyopearl resins, selected for their $DBC_{10\%}$, were evaluated for the purification of human AAT from a clarified CHO-S cell culture (AAT titer: 1.15 mg/mL; HCP titer: 0.5 mg/mL, as found in [63]). A relatively short RT of 2 min was adopted for the binding step to capitalize on the high AAT binding affinity and capacity of the peptidebased adsorbents while attempting to minimize the adsorption of CHO HCPs, as well as increase the productivity of the purification process. As with the control AAT Select resin, the bound AAT was eluted with 2 M MgCl2 in PBS at pH7.4, and the regeneration of the resin was performed under acidic condition (pH 2.5). The chromatograms of AAT purification from the CHO-S CCF are compared in Figure S5; the electrophoretic and SEC analysises of the collected fractions are reported in Fig. 5 and Figure S6; and the resultant values of AAT yield and purity are collated in Table 4.

The electrophoretic analysis of the feedstock highlighted the presence of both monomeric AAT (~54 kDa) and dimeric AAT (~110 kDa; note: dimers resulting from AAT polymerization have been discussed in the literature, [12]); however, while the monomer is consistently found in all eluted fractions, the dimer is uniquely found in the fraction eluted from WHAKKSKFG-Toyopearl resins. Conversely, the SEC chromatograms do not present any peak at ~110 kDa, suggesting that the dimer is non-covalent in nature (and potentially an artifact of the electrophoresis). Despite the small discrepancies, the SDS-PAGE and SEC analysis of the eluted fractions concur in demonstrating that both peptide-based adsorbents bound AAT (i) selectively, with WHAKKSHFG-Toyopearl resin affording a level of AAT purity (92.8%) comparable to that provided by AAT Select resin (97.1%); and (ii) with good capacity, since only minor amounts of AAT could be detected in the flow-through and wash fractions. All resins also eluted AAT efficiently and under mild conditions (2 M MgCl₂ in PBS at pH7.4):

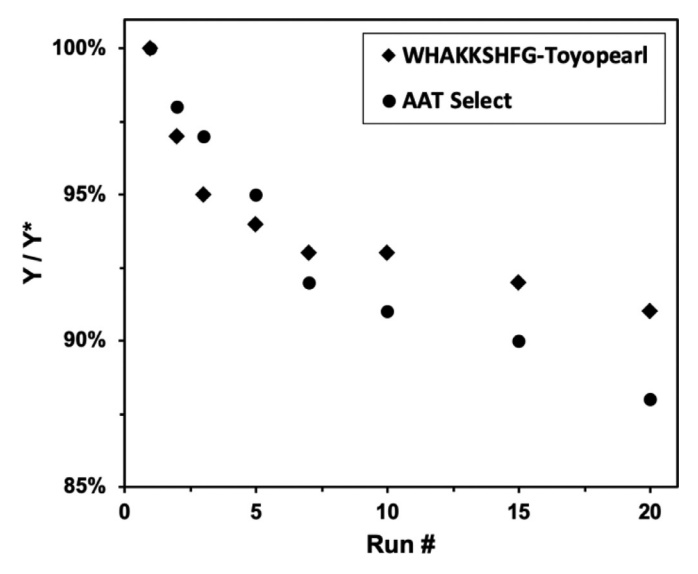


Fig. 6. Lifetime study of WHAKKSHFG-Toyopearl vs. AAT Select resins: values of AAT yield normalized against the AAT yield of the fresh resin measured throughout subsequent cycles of AAT purification, and resin regeneration and alkaline sanitization

WHAKKSKFG- and WHAKKSHFG-Toyopearl resins afforded values of AAT yield of 76.6% and 75.0%, respectively; AAT Select resin performed marginally better, with 79.0%. The AAT not released during elution with MgCl $_2$ was subsequently released during regeneration under acidic conditions. Conversely, KAWFKHWNG-Toyopearl resin afforded a lower AAT purity (\sim 89.1%, data not shown) and insufficient yield (\sim 51.2%); the residual 27.6% of bound AAT was released during CIP.

We finally performed a life-time study of WHAKKSHFG-Toyopearl resin by conducting a series of 20 cycles of AAT purification from CHO CCF using aqueous 0.5 M sodium hydroxide for cleaning the resin following regeneration; caustic sanitization is in fact the industrial standard to ensure safety upon repeated usage of the resin [57]. Notably, we observed a rather minor decrease in the binding capacity and AAT yield provided by WHAKKSHFG-Toyopearl resins with increasing the number of cycles of purification, regeneration, and sanitization (Fig. 6); notably, the peptidebased adsorbent performed comparably to the control AAT Select resin. The exclusion of amino acids prone to alkaline-driven chemical degradation (i.e., asparagine, glutamine, cysteine, methionine) from the peptide sequence and the lack of a tertiary structure characteristic of short peptides make the selected ligand resistant to harsh chemicals, and ensure long lifetime and high reusability of the adsorbent.

4. Conclusions

The extraction of AAT from pooled plasma via precipitation-based fractionation and chromatographic purification has supported augmentation therapy to patients suffering from AATD for decades. The remarkable advancements in the expression of human proteins in engineered CHO cells, combined with the challenges of AAT isolation from plasma, suggest that the future of AAT biomanufacturing may turn towards the recombinant route. This poses an urgent need for affinity adsorbents that combine high binding capacity and selectivity with affordability and scalability. Responding to this challenge, this study introduced a novel affinity adsorbent, WHAKKSHFG-Toyopearl resin, that utilizes a peptide ligand to purify AAT from CHO cell culture harvests. The proposed adsorbent provides comparable product yield and purity, and lifetime compared to its commercial counterpart AAT Select resin,

while surpassing it in terms of binding capacity and affordability. With an estimated cost of \$6K per liter (note: this value is based on the costs of the peptide and the base resin as well as the cost of labor related to the peptide conjugation needed to produce 10 liters of peptide-functionalized adsorbent), WHAKKSHFG-Toyopearl resin is far more convenient than AAT Select (\$15K per liter) [10]. This work plants yet another milestone on the road towards establishing synthetic peptides as affinity ligands for industrial downstream bioprocessing.

Declaration of competing interest

The authors declare no conflict of interest.

CRediT authorship contribution statement

Wenning Chu: Conceptualization, Methodology, Data curation, Writing – original draft. Raphael Prodromou: Methodology, Data curation. Brandyn Moore: Methodology, Data curation. Driss Elhanafi: Methodology, Data curation. Ryan Kilgore: Methodology, Data curation. Shriarjun Shastry: Methodology, Data curation. Stefano Menegatti: Conceptualization, Methodology, Data curation, Writing – review & editing, Funding acquisition.

Acknowledgements

The authors wish to acknowledge the generous support by the Novo Foundation (AIM-Bio Grant NNF19SA0035474) and the National Science Foundation (CBET Award# 1653590).

Supplementary materials

Supplementary material associated with this article can be found, in the online version, at doi:10.1016/j.chroma.2022.463363.

References

- [1] D.H. Perlmutter, Alpha-1-antitrypsin deficiency, Semin. Liver Dis. 18 (3) (1998) 217–225, doi:10.1055/s-2007-1007158.
- [2] M. Cazzola, D. Stolz, P. Rogliani, M.G. Matera, α1-Antitrypsin deficiency and chronic respiratory disorders, Eur. Respiratory Rev. 29 (155) (2020) 190073, doi:10.1183/16000617.0073-2019.
- [3] T. Nakanishi, V. Forgetta, T. Handa, T. Hirai, V. Mooser, G.M. Lathrop, W. Cookson, J.B. Richards, The undiagnosed disease burden associated with alpha-1 antitrypsin deficiency genotypes, Eur. Respir. J. 56 (6) (2020), doi:10.1183/13993003.01441-2020.
- [4] H. Teschler, Long-term experience in the treatment of α 1-antitrypsin deficiency: 25 years of augmentation therapy, Eur. Respir. Rev. 24 (135) (2015) 46–51, doi:10.1183/09059180.10010714.
- [5] S. Viglio, P. Iadarola, M. D'Amato, J. Stolk, Methods of purification and application procedures of alpha1 antitrypsin: a long-lasting history, Molecules 25 (17) (2020), doi:10.3390/molecules25174014.
- [6] P. Kumpalume, A. Podmore, C. LePage, J. Dalton, New process for the manufacture of alpha-1 antitrypsin, J. Chromatogr. A 1148 (1) (2007) 31–37, doi:10.1016/j.chroma.2007.02.068.
- [7] T. Paterson, J. Innes, S. Moore, Approaches to maximizing stable expression of α1-antitrypsin in transformed CHO cells, Appl. Microbiol. Biotechnol. 40 (5) (1994) 691–698, doi:10.1007/BF00173331.
- [8] X. Zhang, Y. Hou, X. Ding, S. Ye, H. Cao, Z. Wang, X. Du, Y.-w. Xie, C. Li, Purification and analysis of human alpha1-antitrypsin concentrate by a new immunoaffinity chromatography, Prep. Biochem. Biotechnol. 44 (7) (2014) 725–737, doi:10.1080/10826068.2013.868358.
- [9] D.Z. Silberstein, in: Process Development and Characterization of a Plant-made, Oxidation Resistant, Recombinant Alpha-1 Antitrypsin, University of California, Davis. Ann Arbor. 2019. p. 154.
- [10] Cytiva, Alpha-1 Antitrypsin select. https://www.cytivalifesciences.com/en/us/ shop/chromatography/resins/affinity-specific-groups/ alpha-1-antitrypsin-select-p-05007. (Accessed 02/07 2022).
- [11] S. Ghose, B. Hubbard, S.M. Cramer, Evaluation and comparison of alternatives to Protein A chromatography: mimetic and hydrophobic charge induction chromatographic stationary phases, J. Chromatogr. A 1122 (1) (2006) 144–152, doi:10.1016/j.chroma.2006.04.083.
- [12] A. Jagger, J.A. Irving, S.T. Rashid, D.A. Lomas, B. Gooptu, Chapter 5 Alpha1-Antitrypsin: structure and dynamics in health, disease and drug development, in: N Kalsheker, R Stockley (Eds.), Alpha-1-antitrypsin Deficiency, Academic Press, Boston, 2017, pp. 49–80, doi:10.1016/B978-0-12-803942-7.00005-2.

- [13] R.A. Lavoie, A. di Fazio, R.K. Blackburn, M.B. Goshe, R.G. Carbonell, S. Menegatti, Targeted capture of chinese hamster ovary host cell proteins: peptide ligand discovery, Int. J. Mol. Sci. 20 (7) (2019) 1729, doi:10.3390/ iims20071729.
- [14] K. Day, R. Prodromou, S. Saberi Bosari, A. Lavoie, M. Omary, C. Market, A. San Miguel, S. Menegatti, Discovery and evaluation of peptide ligands for selective adsorption and release of Cas9 nuclease on solid substrates, Bioconjug. Chem. 30 (12) (2019) 3057–3068, doi:10.1021/acs.bioconjchem.9b00703.
- [15] A. Barozzi, R.A. Lavoie, K.N. Day, R. Prodromou, S. Menegatti, Affibody-binding ligands, Int. J. Mol. Sci. 21 (11) (2020), doi:10.3390/ijms21113769.
- [16] R.A. Lavoie, A. di Fazio, R.G. Carbonell, S. Menegatti, Multiplexed competitive screening of one-bead-one-component combinatorial libraries using a ClonePix 2 colony sorter, Int. J. Mol. Sci. 20 (20) (2019), doi:10.3390/iims20205119.
- [17] Ř. Prodromou, K.N. Day, S. Saberi-Bosari, J.D. Schneible, M.D. Mabe, A. San Miguel, M.A. Daniele, V. Pozdin, S. Menegatti, Engineering next generation cyclized peptide ligands for light-controlled capture and release of therapeutic proteins, Adv. Funct. Mater. 31 (27) (2021) 2101410, doi:10.1002/adfm. 202101410.
- [18] K.S. Lam, S.E. Salmon, E.M. Hersh, V.J. Hruby, W.M. Kazmierski, R.J. Knapp, A new type of synthetic peptide library for identifying ligand-binding activity, Nature 354 (6348) (1991) 82–84, doi:10.1038/354082a0.
- [19] K.S. Lam, V.J. Hruby, M. Lebl, R.J. Knapp, W.M. Kazmierski, E.M. Hersh, S.E. Salmon, The chemical synthesis of large random peptide libraries and their use for the discovery of ligands for macromolecular acceptors, Bioorg. Med. Chem. Lett. 3 (3) (1993) 419–424, doi:10.1016/S0960-894X(01) 80224-9.
- [20] K.S. Lam, D. Lake, S.E. Salmon, J. Smith, M.L. Chen, S. Wade, F. Abdul-Latif, R.J. Knapp, Z. Leblova, R.D. Ferguson, V.V. Krchnak, N.F. Sepetov, M. Lebl, A one-Bead One-Peptide combinatorial library method for B-Cell epitope mapping, Methods 9 (3) (1996) 482–493, doi:10.1006/meth.1996.0056.
- [21] S. Saberi-Bosari, M. Omary, A. Lavoie, R. Prodromou, K. Day, S. Menegatti, A. San-Miguel, Affordable microfluidic bead-sorting platform for automated selection of porous particles functionalized with bioactive compounds, Sci. Rep. 9 (1) (2019) 7210, doi:10.1038/s41598-019-42869-5.
- [22] S. Menegatti, B.G. Bobay, K.L. Ward, T. Islam, W.S. Kish, A.D. Naik, R.G. Carbonell, Design of protease-resistant peptide ligands for the purification of antibodies from human plasma, J. Chromatogr. A 1445 (2016) 93–104, doi:10.1016/j.chroma.2016.03.087.
- [23] T. Bordelon, B. Bobay, A. Murphy, H. Reese, C. Shanahan, F. Odeh, A. Broussard, C. Kormos, S. Menegatti, Translating antibody-binding peptides into peptoid ligands with improved affinity and stability, J. Chromatogr. A 1602 (2019) 284–299, doi:10.1016/j.chroma.2019.05.047.
- [24] H.R. Reese, X. Xiao, C.C. Shanahan, W. Chu, G.A. Van Den Driessche, D. Fourches, R.G. Carbonell, C.K. Hall, S. Menegatti, Novel peptide ligands for antibody purification provide superior clearance of host cell protein impurities, J. Chromatogr. A 1625 (2020) 461237, doi:10.1016/j.chroma.2020. 461237
- [25] W.S. Kish, A.D. Naik, S. Menegatti, R.G. Carbonell, Peptide-based affinity adsorbents with high binding capacity for the purification of monoclonal antibodies, Ind. Eng. Chem. Res. 52 (26) (2013) 8800–8811, doi:10.1021/ie302345w.
- [26] R. Wang, D.-Q. Lin, W.-N. Chu, Q.-L. Zhang, S.-J. Yao, New tetrapeptide ligands designed for antibody purification with biomimetic chromatography: molecular simulation and experimental validation, Biochem. Eng. J. 114 (2016), doi:10.1016/j.bej.2016.06.030.
- [27] G. Madhavi Sastry, M. Adzhigirey, T. Day, R. Annabhimoju, W. Sherman, Protein and ligand preparation: parameters, protocols, and influence on virtual screening enrichments, J. Comput. Aided Mol. Des. 27 (3) (2013) 221–234, doi:10.1007/s10822-013-9644-8.
- [28] M. Rostkowski, M.H.M. Olsson, C.R. Søndergaard, J.H. Jensen, Graphical analysis of pH-dependent properties of proteins predicted using PROPKA, BMC Struct. Biol. 11 (1) (2011) 6, doi:10.1186/1472-6807-11-6.
- [29] M.H.M. Olsson, C.R. Søndergaard, M. Rostkowski, J.H. Jensen, PROPKA3: consistent treatment of internal and surface residues in empirical pKa predictions, J. Chem. Theory Comput. 7 (2) (2011) 525–537, doi:10.1021/ct100578z.
- [30] T. Halgren, New method for fast and accurate binding-site identification and analysis, Chem. Biol. Drug. Des. 69 (2) (2007) 146–148, doi:10.1111/j.1747-0285.
- [31] T.A. Halgren, Identifying and characterizing binding sites and assessing Druggability, J. Chem. Inf. Model. 49 (2) (2009) 377–389, doi:10.1021/ci800324m.
- [32] A. Sharma, V. Tiwari, R. Sowdhamini, Computational search for potential COVID-19 drugs from FDA-approved drugs and small molecules of natural origin identifies several anti-virals and plant products, J. Biosci. 45 (1) (2020) 100, doi:10.1007/s12038-020-00069-8.
- [33] C Tian, K Kasavajhala, K.A.A Belfon, L Raguette, H Huang, A.N Migues, J Bickel, Y Wang, J Pincay, Q Wu, C Simmerling, ff19SB: amino-acid-specific protein backbone parameters trained against quantum mechanics energy surfaces in solution, J. Chem. Theory Comput. 16 (1) (2020) 528–552, doi:10.1021/acs.jctc. 9b00591.
- [34] D.S. Kleinerman, C. Czaplewski, A. Liwo, H.A. Scheraga, Implementations of Nosé-Hoover and Nosé-Poincaré thermostats in mesoscopic dynamic simulations with the united-residue model of a polypeptide chain, J. Chem. Phys. 128 (24) (2008) 245103, doi:10.1063/1.2943146.
- [35] M. Parrinello, A. Rahman, Polymorphic transitions in single crystals: a new molecular dynamics method, J. Appl. Phys. 52 (12) (1981) 7182–7190, doi:10. 1063/1.328693.

- [36] T.E. Cheatham III, J.L. Miller, T. Fox, T.A. Darden, P.A. Kollman, Molecular dynamics simulations on solvated biomolecular systems: the particle mesh Ewald method leads to stable trajectories of DNA, RNA, and proteins, J. Am. Chem. Soc. 117 (14) (1995) 4193–4194, doi:10.1021/ja00119a045.
- [37] R.V. Honorato, P.I. Koukos, B. Jiménez-García, A. Tsaregorodtsev, M. Verlato, A. Giachetti, A. Rosato, A.M.J.J. Bonvin, Structural biology in the clouds: the WeNMR-EOSC ecosystem, Front. Mol. Biosci. 8 (2021), doi:10.3389/fmolb.2021. 729513.
- [38] G.C.P. van Zundert, J.P.G.L.M. Rodrigues, M. Trellet, C. Schmitz, P.L. Kastritis, E. Karaca, A.S.J. Melquiond, M. van Dijk, S.J. de Vries, A.M.J.J. Bonvin, The HAD-DOCK2.2 web server: user-friendly integrative modeling of biomolecular complexes, J. Mol. Biol. 428 (4) (2016) 720–725, doi:10.1016/j.jmb.2015.09.014.
- [39] D. Spiliotopoulos, P.L. Kastritis, A.S. Melquiond, A.M. Bonvin, G. Musco, W. Rocchia, A. Spitaleri, dMM-PBSA: a New HADDOCK scoring function for protein-peptide docking, Front. Mol. Biosci. 3 (2016) 46, doi:10.3389/fmolb.2016. 00046
- [40] H. Loebermann, R. Tokuoka, J. Deisenhofer, R. Huber, Human α 1-proteinase inhibitor: crystal structure analysis of two crystal modifications, molecular model and preliminary analysis of the implications for function, J. Mol. Biol. 177 (3) (1984) 531–557, doi:10.1016/0022-2836(84)90298-5.
- [41] P.E. Stein, A.G.W. Leslie, J.T. Finch, W.G. Turnell, P.J. McLaughlin, R.W. Carrell, Crystal structure of ovalbumin as a model for the reactive centre of serpins, Nature 347 (6288) (1990) 99–102, doi:10.1038/347099a0.
- [42] P.R. Elliott, D.A. Lomas, R.W. Carrell, J.P. Abrahams, Inhibitory conformation of the reactive loop of alpha 1-antitrypsin, Nat. Struct. Biol. 3 (8) (1996) 676–681, doi:10.1038/nsb0896-676.
- [43] J.A. Huntington, R.J. Read, R.W. Carrell, Structure of a serpin-protease complex shows inhibition by deformation, Nature 407 (6806) (2000) 923–926, doi:10. 1038/35038119.
- [44] D.A. Johnson, J. Travis, Human alpha-1-proteinase inhibitor mechanism of action: evidence for activation by limited proteolysis, Biochem. Biophys. Res. Commun. 72 (1) (1976) 33–39, doi:10.1016/0006-291x(76)90956-6.
- [45] I. Schechter, A. Berger, On the size of the active site in proteases. I. Papain, Biochemical and biophysical research communications 27(2) (1967) 157–62. 10.1016/s0006-291x(67)80055-x.
- [46] NORDAlpha-1 Antitrypsin Deficiency, 2022 https://rarediseases.org/ rare-diseases/alpha-1-antitrypsin-deficiency/ (Accessed 02/07).
- [47] M.D. Hanwell, D.E. Curtis, D.C. Lonie, T. Vandermeersch, E. Zurek, G.R. Hutchison, Avogadro: an advanced semantic chemical editor, visualization, and analysis platform, J. Cheminform. 4 (1) (2012) 17, doi:10.1186/1758-2946-4-17.
- [48] L.R. English, E.C. Tilton, B.J. Ricard, S.T. Whitten, Intrinsic α helix propensities compact hydrodynamic radii in intrinsically disordered proteins, Proteins Struct. Funct. Bioinf. 85 (2) (2017) 296–311, doi:10.1002/prot.25222.
- [49] L. Andersson, L. Blomberg, M. Flegel, L. Lepsa, B. Nilsson, M. Verlander, Large-scale synthesis of peptides, Pept. Sci. 55 (3) (2000) 227–250, doi:10.1002/1097-0282(2000)55:3(227:AID-BIP50)3.0.CO;2-7.
- [50] B.L. Bray, Large-scale manufacture of peptide therapeutics by chemical synthesis, Nat. Rev. Drug Discov. 2 (7) (2003) 587–593 https://www.nature.com/articles/prd1133
- [51] S. Menegatti, A.D. Naik, R.G. Carbonell, The hidden potential of small synthetic molecules and peptides as affinity ligands for bioseparations, Pharm. Bioprocess. 1 (5) (2013) 467-485 https://www.openaccessjournals.com/abstract/ the-hidden-potential-of-small-synthetic-molecules-and-peptides-as-affinityligands-for-bioseparations-8112.html.
- [52] H.R. Reese, C.C. Shanahan, C. Proulx, S. Menegatti, Peptide science: a "rule model" for new generations of peptidomimetics, Acta Biomater. 102 (2020) 35–74, doi:10.1016/j.actbio.2019.10.045.
- [53] M. Lebl, V. Krchňák, S.E. Salmon, K.S. Lam, Screening of completely random one-bead one-peptide libraries for activities in solution, Methods 6 (4) (1994) 381–387, doi:10.1006/meth.1994.1038.
- [54] O.H. Aina, R. Liu, J.L. Sutcliffe, J. Marik, C.-X. Pan, K.S. Lam, From combinatorial chemistry to cancer-targeting peptides, Mol. Pharm. 4 (5) (2007) 631–651, doi:10.1021/mp700073y.
- [55] W.S. Kish, H. Sachi, A.D. Naik, M.K. Roach, B.G. Bobay, R.K. Blackburn, S. Menegatti, R.G. Carbonell, Design, selection, and development of cyclic peptide ligands for human erythropoietin, J. Chromatogr. A 1500 (2017) 105–120, doi:10.1016/j.chroma.2017.04.019.
- [56] W.S. Kish, M.K. Roach, H. Sachi, A.D. Naik, S. Menegatti, R.G. Carbonell, Purification of human erythropoietin by affinity chromatography using cyclic peptide ligands, J. Chromatogr. B 1085 (2018) 1–12, doi:10.1016/j.jchromb.2018.03.039.
- [57] S. Menegatti, A.D. Naik, P.V. Gurgel, R.G. Carbonell, Alkaline-stable peptide ligand affinity adsorbents for the purification of biomolecules, J. Chromatogr. A 1245 (2012) 55–64, doi:10.1016/j.chroma.2012.04.072.
- [58] K. Day, J.D. Schneible, A.T. Young, V.A. Pozdin, G. Van Den Driessche, L.A. Gaffney, R. Prodromou, D.O. Freytes, D. Fourches, M. Daniele, S. Menegatti, Photoinduced reconfiguration to control the protein-binding affinity of azobenzene-cyclized peptides, J. Mater. Chem. B 8 (33) (2020) 7413–7427, doi:10.1039/DOTB01189D.
- [59] R.P. Mukherjee, S. Menegatti, P.V. Gurgel, R.G. Carbonell, B.G. Bobay, Exploration of the binding mechanism of trimeric peptide ligands for the purification of butryrlcholinesterase, Biotechnol. Bioegineering (submitted) (2022).
- [60] J. Knezevic, A. Langer, P.A. Hampel, W. Kaiser, R. Strasser, U. Rant, Quantitation of affinity, avidity, and binding kinetics of protein analytes with a dynamically switchable Biosurface, J. Am. Chem. Soc. 134 (37) (2012) 15225–15228, doi:10. 1021/ja3061276.

- [61] S. Merminod, J.R. Edison, H. Fang, M.F. Hagan, W.B. Rogers, Avidity and surface mobility in multivalent ligand–receptor binding, Nanoscale 13 (29) (2021) 12602–12612, doi:10.1039/D1NR02083H.
- [62] E. Campbell, L. Scott, Quantitative isoelectric focusing of alpha1-antitrypsin: grouping and prevalence of unusual alpha1-antitrypsin variants, Chest 144 (4) (2013) 705A https://journal.chestnet.org/article/S0012-3692(16)43339-8/fulltext#relatedArticles .
- [63] T. Amann, A.H. Hansen, S. Kol, H.G. Hansen, J. Arnsdorf, S. Nallapareddy, B. Voldborg, G.M. Lee, M.R. Andersen, H.F. Kildegaard, Glyco-engineered CHO cell lines producing alpha-1-antitrypsin and C1 esterase inhibitor with fully humanized N-glycosylation profiles, Metab. Eng. 52 (2019) 143–152, doi:10.1016/j.ymben.2018.11.014.